

Load Network Design Technique for Class F and Inverse Class F PAs

By Andrei Grebennikov
 Bell Labs, Alcatel-Lucent

This article explains the design procedure for implementing a practical output network for Class-F and inverse Class-F power amplifiers

Highly efficient operation of the power amplifier can generally be obtained by applying bi-harmonic or polyharmonic modes, when an additional single-resonant or multi-resonant circuit tuned to the odd or even harmonics of the fundamental frequency is added into the load network. An infinite number of odd-harmonic resonators results in an idealized Class F mode with a square voltage waveform and a half-sinusoidal current waveform at the device output terminal, while an infinite number of even-harmonic resonators results in an idealized inverse Class F mode with a half-sinusoidal voltage waveform and a square current waveform at the device output terminal [1, 2]. In conventional Class F or inverse Class F power amplifiers analyzed in frequency domain, the fundamental and harmonic load-network impedances are optimized by short-circuit termination and open-circuit peaking to control the voltage and current waveforms at the device output to obtain maximum efficiency. They are equal respectively to

$$Z_{\text{net}}(\omega_0) = R = \frac{8 V_{\text{cc}}}{\pi^2 I_0} \text{ or } \frac{\pi^2 V_{\text{cc}}}{8 I_0} \quad (1)$$

$$Z_{\text{net}}(2n\omega_0) = 0 \quad (2)$$

(or ∞ for even harmonics)

$$Z_{\text{net}}[(2n+1)\omega_0] = \infty \quad (3)$$

(or 0 for odd harmonics)

where R is the fundamental-frequency load-network impedance (or optimum load-line

resistance), V_{cc} is the supply voltage, and I_0 is the dc current component.

Idealized Waveforms with Sinewave Drive

In an ideal Class B operation mode with output parallel resonant circuit tuned to the fundamental frequency, the maximum theoretical anode (collector or drain) efficiency achieves only 78.5% characterized by the sinusoidal anode voltage waveform and half-sinusoidal current waveform. To increase efficiency up to maximum theoretical value of 100%, additional resonators must be included into the load network, each of which is tuned to the corresponding harmonic component. In the case of an infinite number of harmonic resonators and an active device considered an ideal lossless switch, this can result in an output half-sinusoidal current waveform and a square voltage waveform (Class F mode), and an output half-sinusoidal voltage waveform and a square current waveform (inverse Class F, or Class F⁻¹ mode). In this case, a Fourier series for the corresponding output current $i(t)$ and voltage $v(t)$ in normalized forms can be written as

$$\left. \frac{i(\omega t)}{I_0} \right|_{\text{Class F}} = \left. \frac{v(\omega t)}{V_0} \right|_{\text{Class F}^{-1}} = 1 - \frac{\pi}{2} \sin \omega t - 2 \sum_{n=2,4,6,\dots}^N \frac{\cos n\omega t}{n^2 - 1} \quad (4)$$

$$\left. \frac{v(\omega t)}{V_0} \right|_{\text{Class F}} = \left. \frac{i(\omega t)}{I_0} \right|_{\text{Class F}^{-1}} = 1 + \frac{4}{\pi} \sin \omega t + \frac{4}{\pi} \sum_{n=3,5,7,\dots}^N \frac{\sin n\omega t}{n} \quad (5)$$

acterized by more than 3-dB gain compression point. Due to the diode-based nonlinearity of the device input circuit, the amplitude harmonic ratio between the fundamental-frequency, second, and third harmonic components at the gate terminal is 8.2:1.3:1.

An idealized inverse Class F oper-

ation mode can be represented by using a series quarterwave transmission line loaded by the series resonant circuit tuned to the fundamental frequency [2, 4]. Figure 3 shows the circuit schematic of an inverse Class F power amplifier with a series quarterwave line based on a 28-V 10-W Cree GaN HEMT power transistor

CGH40010. In this case, the series-tuned output circuit presents to the transmission line a load resistance at the frequency of operation. For even harmonics, the open circuit on the load side of the transmission line is repeated, thus producing an open circuit at the drain. However, the quarterwave transmission line converts the open circuit at the load to a short circuit at the drain for odd harmonics with resistive load at the fundamental frequency.

Similarly to the Class F GaN HEMT power amplifier, a simple lossy RL input shunt network is also used to match the device input impedance to a 50 Ω source and to compensate for the device input gate-source capacitance $C_{in} = 5$ pF at the fundamental frequency, providing a small-signal S_{11} better than 20 dB at an operating frequency of 200 MHz. The series 55 Ω resistor is necessary to provide unconditional operation stability. The simulated drain voltage (close to half-sinusoidal blue curve) and current (close to square red curve) waveforms are shown in Fig. 4(a) where small deviations from the ideal waveforms (with optimized load-network parameters) can be

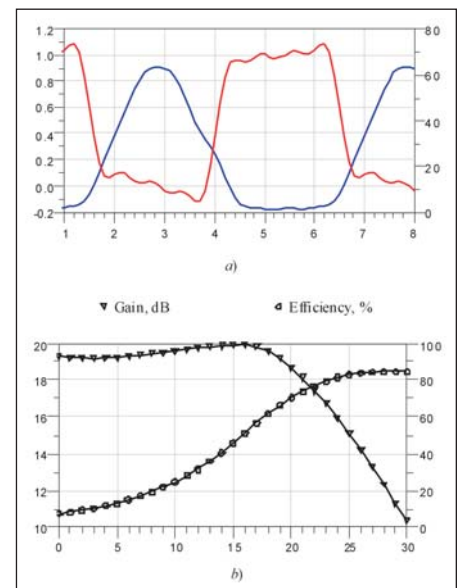


Figure 4 . Simulated waveforms, gain and efficiency of inverse Class F GaN HEMT power amplifier.

explained due to effect of the device output drain-source capacitance C_{out} and package parasitics. In this case, a maximum drain efficiency of 84.8% with a power gain of 12.3 dB and an output power of 40.3 dBm at a supply voltage of 24 V were obtained with a sine-wave driving signal in a deep saturation condition, as shown in Fig. 4(b).

Basic Practical Load Network Configurations

In practice, it is usually enough to apply the second- or third-harmonic peaking to achieve maximum drain efficiency of more than 80% in Class F or inverse Class F mode that can result in a sufficiently simple circuit schematic convenient for practical realization [5, 6]. For example, by providing a proper high-impedance second-harmonic peaking and load matching at the fundamental, the collector efficiency of 83% was achieved for a 435-MHz microstrip power amplifier [7]. Generally, the optimum impedance matching at the fundamental frequency with the second- and third-harmonic tuning can be provided by using the series transmission-line sections and shunt open-circuit stubs to obtain open-circuit peaking and short-circuit termination seen by the device output at corre-

sponding harmonic component [8, 9].

Figure 5(a) shows the idealized basic configuration of the transmission-line Class F load network where a shunt quarter-wavelength transmission line providing a short-circuit termination for even voltage harmonic at the device output is connected to the dc power supply with bypass

capacitor. The series transmission-line section and open-circuit stub, both having an electrical length of 30° at the fundamental frequency, provide an open-circuit mode at the third harmonic because an open-circuit stub has a quarter wavelength at the third harmonic to realize a short-circuit condition at the right-hand side

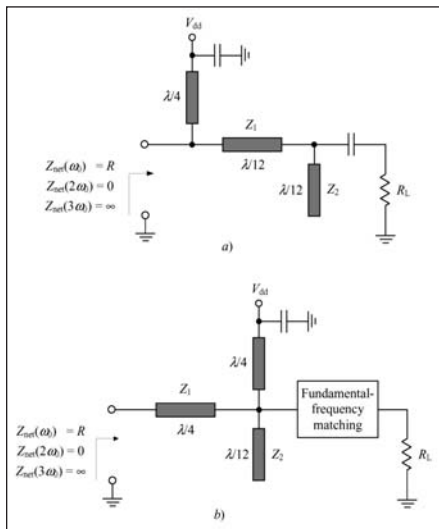


Figure 5 . Idealized transmission-line Class F load networks.

of the series transmission line having a quarter wavelength at the third harmonic as well. Such a Class F load network implemented using coplanar lines into a 24-GHz MMIC GaAs pHEMT power amplifier had contributed to a drain efficiency of 59% at an output power of 20 dBm [10].

The load-network impedance Z_{net} seen by the device output at the fundamental frequency can be written as

$$Z_{net} = Z_1 \frac{R_L (Z_2 - Z_1 \tan^2 \theta) + jZ_1 Z_2 \tan \theta}{Z_1 Z_2 + j(Z_1 + Z_2) R_L \tan \theta} \quad (6)$$

where $\theta = \theta_1 = \theta_2 = 30^\circ$, Z_1 and θ_1 are the characteristic impedance and electrical length of the series transmission line, and Z_2 and θ_2 are the characteristic impedance and electrical length of the open-circuit stub. Hence, the impedance matching with the load at the fundamental can be provided by proper choice of the characteristic impedances Z_1 and Z_2 .

Separating Eq. (6) into real and imaginary parts and taking into account that $\text{Re}Z_{net} = R$ and $\text{Im}Z_{net} = 0$, the system of two equations with two unknown parameters is obtained by

$$Z_1^2 Z_2^2 - R_L^2 (Z_1 + Z_2) (Z_2 - Z_1 \tan^2 \theta) = 0 \quad (7)$$

$$(Z_1 + Z_2)^2 R_L^2 \tan^2 \theta - Z_1^2 Z_2^2 [R_L (1 + \tan^2 \theta) - R] = 0 \quad (8)$$

which enables the characteristic impedances Z_1 and Z_2 to be properly calculated. This system of two equations can be explicitly solved as a function of the parameter $r = R_L/R$ resulting in

$$\frac{Z_1}{R_L} = \frac{\sqrt{4r - 3}}{r} \quad (9)$$

$$\frac{Z_1}{Z_2} = 3 \left(\frac{r-1}{r} \right) \quad (10)$$

Consequently, for the specified value of the parameter r with the required Class F optimum fundamental-frequency load resistance R and standard load resistance $R_L = 50 \Omega$, the characteristic impedance Z_1 is calculated from Eq. (9) and then the characteristic impedance Z_2 is calculated from Eq. (10). For example, if the required Class F optimum load resistance R is equal to 12.5 Ω resulting in $r = 4$, the characteristic impedance of the series transmission line Z_1 is equal to 45 Ω and the characteristic impedance of the open-circuit stub Z_2 is equal to 20 Ω .

Figure 5(b) shows the simplified Class F load network with the second- and third-harmonic tuning using a series quarter-wavelength transmission line which pro-

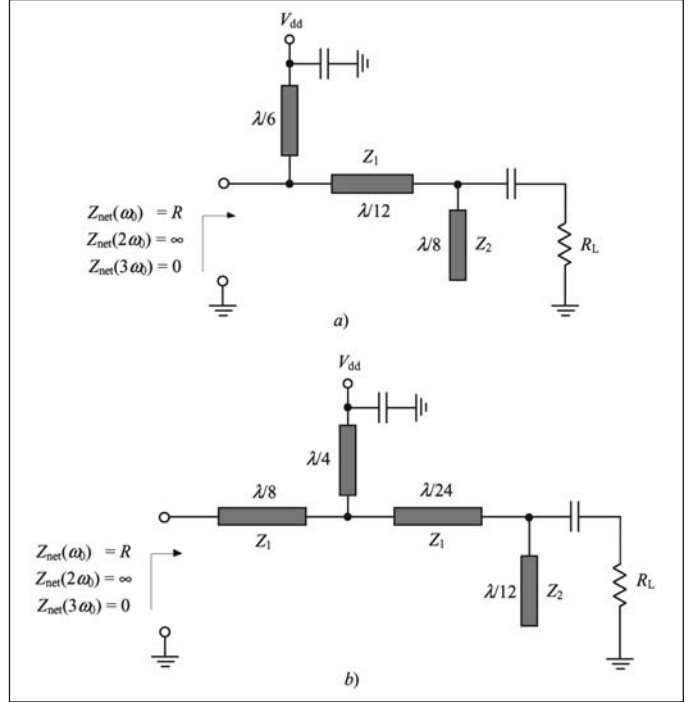


Figure 6 · Idealized transmission-line inverse Class F load network.

vides zero impedance at the second harmonic and infinite impedance at the third harmonic components [11]. The short-circuit impedances at right-hand side of the series quarter-wavelength transmission line is provided by a short-circuited shunt quarter-wavelength transmission line at the second harmonic and an open-circuit $\lambda/12$ stub at the third harmonic. In this case, to provide an impedance matching at the fundamental frequency, it is necessary to use a separate matching circuit since the series quarter-wavelength transmission line with characteristic impedance Z_1 can match only real part of the equivalent fundamental-frequency device output impedance equal to Class F optimum load resistance R . However, there is no additional parameter to compensate for its imaginary part.

Figure 6(a) shows the idealized transmission-line inverse Class F load-network schematic where a shunt $\lambda/6$ transmission line grounded through the bypass capacitor provides low impedance for the third harmonic and certain impedances for the fundamental and second harmonics at the de-vice drain terminal [2, 12]. The second-harmonic peaking is achieved by using an open-circuit $\lambda/8$ stub which creates a low impedance at the right-hand side of the series $\lambda/12$ transmission line at the second harmonic. As a result, this series $\lambda/12$ transmission line with electrical length of 60° at the second harmonic (combined in parallel with the shunt $\lambda/6$ transmission line with electrical length of 120° at the second harmonic) represents a

second-harmonic tank.

It is also useful and very practical for inverse Class F power amplifiers to consider an alternative transmission-line inverse Class F load network with a series $\lambda/8$ transmission line as a first element, as shown in Fig. 6(b) [13]. In this case, the series $\lambda/8$ transmission line short-circuited at its right-hand side by the shunt quarter-wavelength transmission line at the second harmonic provides an open circuit at the second harmonic seen by the device output, while the combined $(\lambda/8 + \lambda/24 = \lambda/6)$ series transmission line short-circuited at its right-hand side by the open-circuit $\lambda/12$ stub provides a short circuit at the third harmonic seen by the device output.

The load-network impedance Z_{net} at the fundamental can be written similarly to Eq. (6) as

$$Z_{net} = Z_1 \frac{R_L (Z_2 - Z_1 \tan 30^\circ \tan 60^\circ) + jZ_1 Z_2 \tan 60^\circ}{Z_1 Z_2 + j(Z_1 \tan 30^\circ + Z_2 \tan 60^\circ) R_L} \quad (11)$$

where Z_1 is the characteristic impedance of the combined series transmission line and Z_2 is the characteristic impedance of an open-circuit $\lambda/12$ stub. Separating Eq. (11) into real and imaginary parts, the system of two equations with two unknown parameters is obtained by

$$(Z_1 + 3Z_2)^2 R_L^2 R - 3Z_1^2 Z_2^2 (4R_L - 3R) = 0 \quad (12)$$

$$3Z_1^2 Z_2^2 - R_L^2 (Z_2 - Z_1)(Z_1 + 3Z_2) = 0 \quad (13)$$

which allows direct calculation of the characteristic impedances Z_1 and Z_2 . This system of two equations can be explicitly solved as a function of the parameter $r = R_L/R$ resulting in

$$\frac{Z_1}{R_L} = \frac{\sqrt{4r-1}}{\sqrt{3}r} \quad (14)$$

$$\frac{Z_1}{Z_2} = \frac{r-1}{r} \quad (15)$$

Consequently, if the required optimum load resistance and standard load resistance are equal to $R = 20 \Omega$ and $R_L = 50 \Omega$, respectively, resulting in $r = 2.5$, then the characteristic impedance of the series transmission line calculated from Eq. (12) is equal to $Z_1 = 35 \Omega$ and the characteristic impedance of the open circuit stub calculated from Eq. (13) is equal to $Z_2 = 58 \Omega$.

Load Network with Stepped-Impedance Transmission Line

As it follows from Fig. 5(b), if it is enough to use a single series quarter-wavelength transmission line to pro-

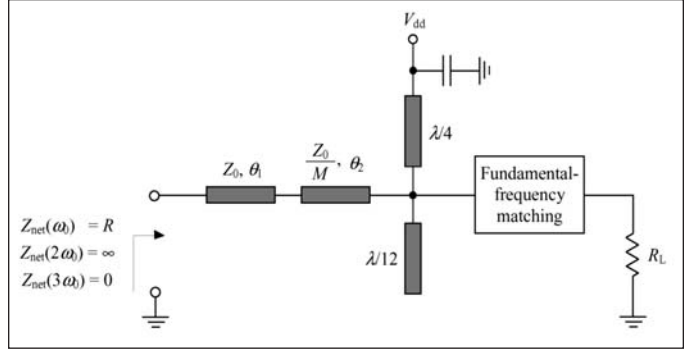


Figure 7 · Idealized transmission-line inverse Class F load network.

vide a short circuit at the second harmonic and open circuit at the third harmonic in a Class F mode, then it is necessary to use a series $\lambda/8$ line to provide an open circuit at the second harmonic and a series $\lambda/6$ line to provide a short circuit at the third harmonic in an inverse Class F mode. To combine effects of these two uniform transmission lines, the non-uniform stepped-impedance transmission line can be used. It is known that the band properties of a resonant circuit containing a short-circuited transmission line can be improved if, instead of a uniform transmission line, a non-uniform transmission line is used, the spectrum of natural frequencies of which is much non-equidistant [14, 15]. Among the resonant systems with non-uniform transmission lines, the resonant systems with multi-section line having alternating high and low characteristic impedances of its uniform sections are ideal from the standpoint of maximum frequency tuning bandwidth. A sensitivity variation of such a multi-section line is determined by a spectrum rarefaction near resonant frequency for a tuning band widening and spectrum narrowing in the case of frequency stabilization. In this case, a simple combination of two loaded transmission lines with high and low characteristic impedances can provide the fundamental impedance matching and second-harmonic tuning to a high impedance nearby open condition simultaneously [16].

Figure 7 shows the simplified inverse Class F load network with the second and third harmonic tuning using a series stepped-impedance transmission line which can provide infinite impedance at the second harmonic and zero impedance at the third harmonic components, where θ_1 and θ_2 are the electrical lengths of the stepped-impedance transmission-line sections and M is the characteristic impedance ratio. Using the shunt quarter-wavelength transmission line is convenient to directly supply dc current to the active device from the power supply since it is RF grounded at its end. For the simplicity of analytical calculations, the transmission-line lengths can be set equal as $\theta = \theta_1 = \theta_2$.

The input network impedance Z_{net} as a function of electrical length θ of equal sections of the stepped-impedance transmission line is written as

$$Z_{net} = Z_0 \frac{Z_L(1 - M \tan^2 \theta) + jZ_0 \left(\frac{1}{M} + 1 \right) \tan \theta}{Z_0 \left(1 - \frac{\tan^2 \theta}{M} \right) + jZ_L(M + 1) \tan \theta} \quad (16)$$

where Z_L is the load impedance including the short-circuit and open-circuit stubs.

For $Z_L = 0$,

$$Z_{net} = jZ_0 \frac{\frac{1}{M} + 1}{1 - \frac{\tan^2 \theta}{M}} \tan \theta \quad (17)$$

whose zeroes correspond to $\theta_{0k} = (\pi/2)k$ and poles correspond to

$$\theta_{pk} = k\pi \pm \tan^{-1} \sqrt{M} \quad (18)$$

where $k = 0, 1, 2, \dots$. Thus, by choosing the proper characteristic impedance ratio M , the first pole θ_{p1} can be moved from initial value of 45° for uniform line towards the second zero at $\theta_{02} = 90^\circ$ and set at $\theta_{p1} = 60^\circ$ for the stepped-impedance transmission line with $M = 3$. As a result, by using such a stepped-impedance transmission line, an open circuit at the second harmonic and short circuit at the third harmonic of the fundamental frequency can be provided if the fundamental frequency corresponds to $\theta = 30^\circ$.

Figure 8(a) shows the design example of a stepped-impedance transmission-line inverse Class F load network with harmonic tuning which provides an impedance matching at the fundamental frequency between the input impedance of 20Ω and load impedance of 50Ω at an operating frequency $f_0 = 2 \text{ GHz}$. In this case, the stepped-impedance transmission line with equal section lengths of 30° loaded by the short-circuited quarter-wavelength line and open-circuit $\lambda/12$ stub creates an open circuit at the second harmonic and short circuit at the third harmonic seen by the $20\text{-}\Omega$ source at its input. Using of a subsequent short-length transmission line as an element of the output fundamental-frequency matching circuit is required to compensate for the reactive part of the modified source impedance (any source impedance can be transformed to a real load impedance using a $\lambda/8$ transformer whose characteristic impedance is equal to the magnitude of the source impedance [17]) followed by the quarter-wavelength transmission line which provides the transformation of the real part of the modified source impedance to the standard load of 50Ω . The frequency

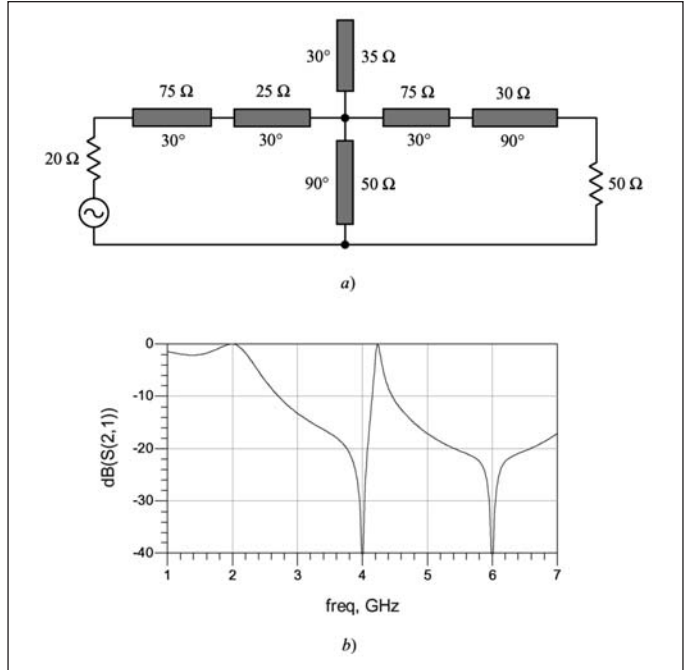


Figure 8 · Frequency response of load network with second- and third-harmonic tuning.

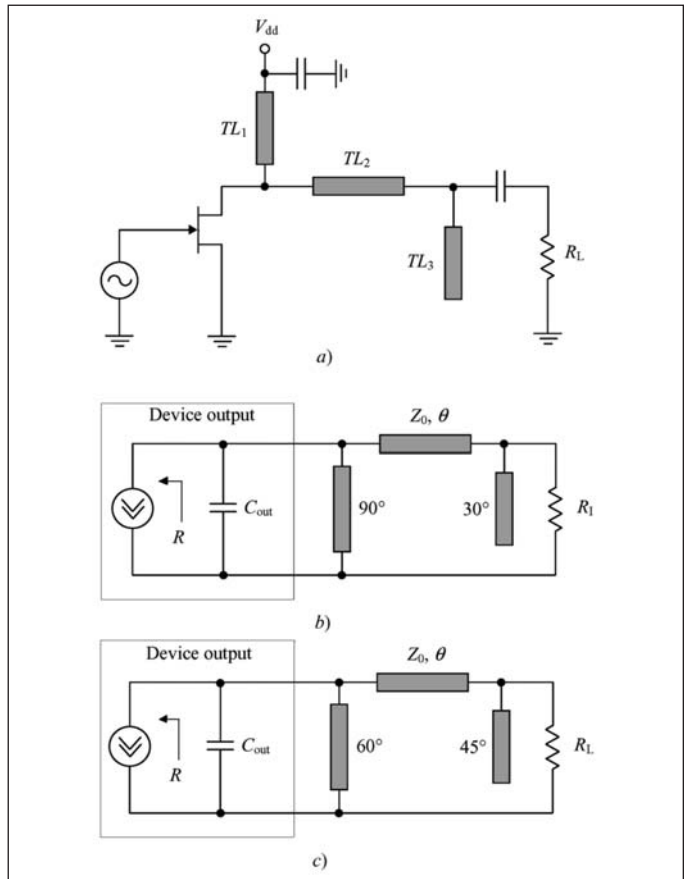


Figure 9 · Transmission-line load networks with shunt capacitance.

response of such a stepped-impedance transmission-line inverse Class F load network with harmonic tuning is shown in Fig. 8(b), which demonstrates the fundamental-frequency impedance matching at 2 GHz, second-harmonic open circuit at 4 GHz, and third-harmonic short circuit at 6 GHz.

Effect of Shunt Capacitance

However, the efficiency of the power amplifier can be limited by the transistor output capacitance C_{out} (mostly represented by drain-source capacitance C_{ds} or collector capacitance C_c) if this capacitance is not absorbed into multiharmonic load network without compromising the ability to properly terminate the second and third harmonic components. Figure 9(a) shows the simplified circuit schematic of the transmission-line transistor power amplifier, whereas the equivalent load network corresponding to Class F mode with a shunt short-circuited quarter-wavelength transmission line which provides a short circuit at even harmonics is shown in Fig. 9(b) and equivalent load network corresponding to inverse Class F mode with a shunt short-circuited $\lambda/3$ transmission line which provides a short circuit at the third harmonic at the device output is shown in Fig. 9(c).

In Class F mode with a load network shown in Fig. 9(b), the electrical length of an open-circuit stub TL_3 is chosen to have a quarter wavelength at the third harmonic to realize short-circuit condition at the right-hand side of the series transmission line TL_2 , whose electrical length θ should provide an inductive reactance to resonate with the device output capacitance C_{out} at the third harmonic. Such a load network is very practical when the dc drain voltage is very high to increase the device output impedance, or operating frequency is sufficiently low, and bare die is used instead of packaged transistor to easily absorb bondwire inductances by the load network [18]. In inverse Class F mode with a load network shown in Fig. 9(c), both transmission lines TL_1 and TL_2 having overall inductive reactance in a parallel connection are tuned to the parallel resonance condition with the device output capacitance C_{out} to form a parallel resonant circuit to realize an open-circuit condition for the second harmonic at the device output [2].

As a result, the electrical lengths of the series transmission line TL_2 at the fundamental frequency can be obtained by

$$\theta = \frac{1}{3} \tan^{-1}(2Z_0\omega_0 C_{out}) \quad \text{for Class F} \quad (19)$$

$$\theta = \frac{1}{2} \tan^{-1} \left[\left(2Z_0\omega_0 C_{out} + \frac{1}{\sqrt{3}} \right)^{-1} \right] \quad \text{for Class F}^{-1} \quad (20)$$

where Z_0 is the characteristic impedance of the series trans-

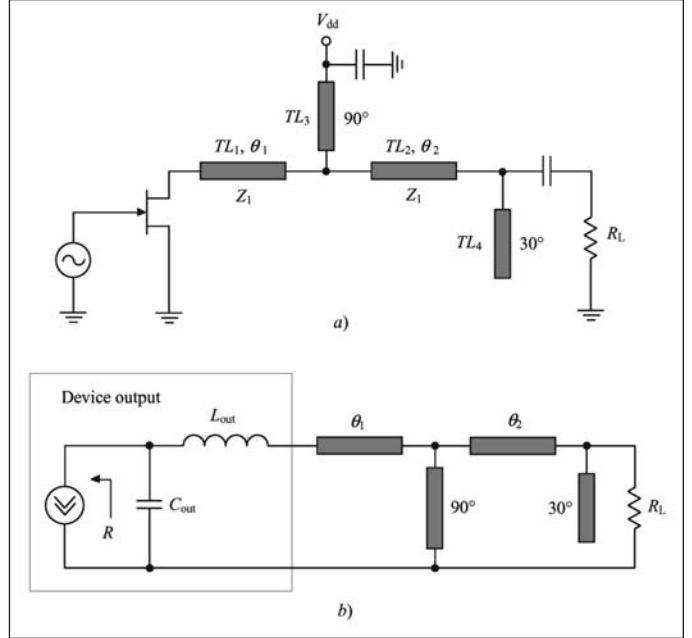


Figure 10 · Transmission-line inverse Class F power amplifier and its equivalent circuit.

mission line TL_2 and ω_0 is the fundamental frequency.

However, when effect of the device output parasitic series inductance becomes significant, it leads to an additional circuit complexity and some problems with tuning accuracy. In this case, it is possible to use either an additional series compensation line [19] or an additional open-circuit transmission-line stub [20] that generally results in excessive losses at harmonic frequencies and lower efficiency.

Effect of Series Inductance

In a power amplifier using the packaged device at high frequencies or with high output power, the presence of a transistor output series bondwire and lead inductance L_{out} creates some problems in providing an acceptable second- or third-harmonic open- or short-circuit termination. Even if L_{out} can be placed between the device output capacitance C_{out} and shunt short-circuited transmission line TL_1 shown in Fig. 9(a) and a short-circuit termination is provided at its right-hand side, the open-circuit condition will fully depend on a physical length of this inductance which is difficult to set very accurately in practical hybrid or monolithic integrated circuits.

In this case, it is convenient to use a series transmission line as a first element of the load network connected to the device output, as shown in Fig. 10(a), where the transmission line TL_1 is placed between the device drain terminal and shunt short-circuited quarter-wavelength transmission line TL_3 . However, if in a Class F mode with short circuit at the second harmonic and open circuit at

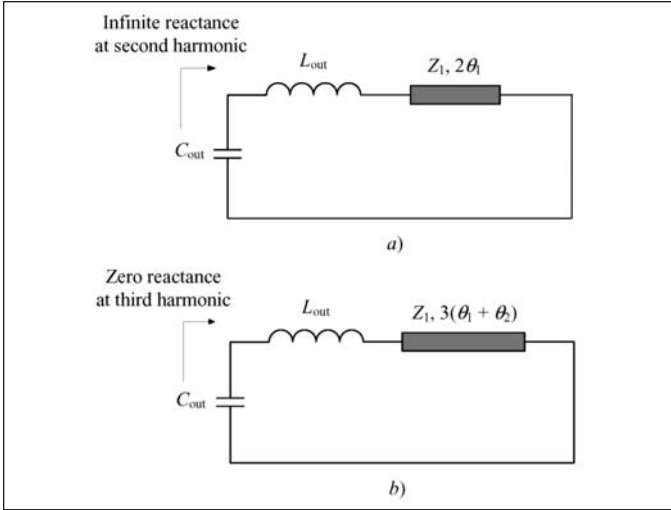


Figure 11 · Load networks seen by the device output at second and third harmonics.

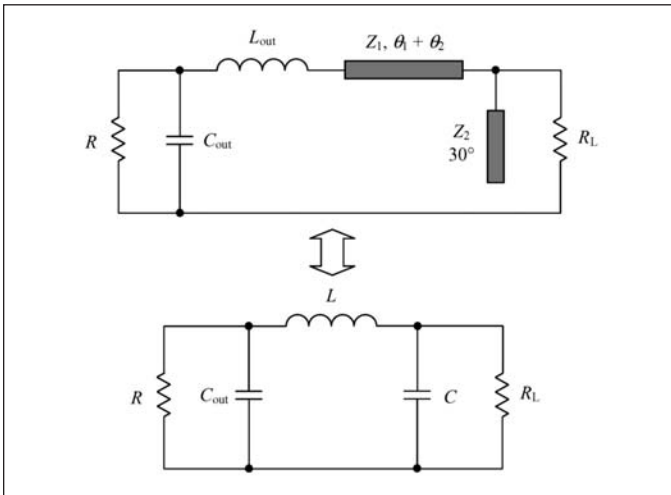


Figure 12 · Equivalent representations of load network at fundamental frequency.

the third harmonic, the length of combined series transmission line $TL_1 + TL_2$ becomes very long and additional fundamental-frequency matching circuit is required, then such a load network in an inverse Class F mode is compact, convenient for harmonic tuning, and very practical. Figure 10(b) shows the transmission-line inverse Class-F load network, where the combined series transmission line $TL_1 + TL_2$ (together with an open-circuit capacitive stub TL_4 with electrical length of 30°) provides an impedance matching between optimum fundamental-frequency load resistance R and standard load resistance R_L by proper choice of the transmission-line characteristic impedances Z_1 and Z_2 , where C_{out} and L_{out} are the elements of the matching circuit [21].

The load network seen by the device multiharmonic

current source at the second harmonic is shown in Fig. 11(a), with shorting effect of the quarterwave short-circuited stub TL_3 . Here, the series transmission line TL_1 provides an open-circuit condition for the second harmonic at the device output by forming a second-harmonic tank together with C_{out} and L_{out} . Similar load network at the third harmonic is shown in Fig. 11(b), due to the open-circuit effect of the short-circuited quarter-wave line TL_3 and shorting effect of the open-circuit stub TL_4 at the third harmonic. In this case, the combined transmission line $TL_1 + TL_2$ (together with the series inductance L_{out}) provides a short-circuit condition for the third harmonic at the device output being shorted at its right-hand side. The electrical lengths of the transmission lines TL_1 and TL_2 , assuming the same characteristic impedance Z_1 for both series transmission-line sections, can be defined from

$$2\omega_0 C_{out} - \frac{1}{2\omega_0 L_{out} + Z_1 \tan 2\theta_1} = 0 \quad (21)$$

$$3\omega_0 L_{out} + Z_1 \tan 3(\theta_1 + \theta_2) = 0 \quad (22)$$

with the maximum total electrical length $\theta_1 + \theta_2 = \pi/3$ or 60° at the fundamental frequency or 180° at the third harmonic component when $L_{out} = 0$.

Figure 12 shows the equivalent representation of an inverse Class F load network (including the device output parameters L_{out} and C_{out}) by a lumped low-pass π -type matching circuit where

$$C = \tan 30^\circ / (\omega_0 Z_2)$$

$$L \cong (Z_1 / \omega_0) \sin(\theta_1 + \theta_2) + L_{out}$$

due to the sufficiently short length of the combined transmission line $TL_1 + TL_2$, typically much less than 60° at the fundamental frequency depending on the device output parameters. As a result,

$$Z_1 \cong \frac{\omega_0 (L - L_{out})}{\sin(\theta_1 + \theta_2)} \quad (23)$$

$$Z_2 = \frac{1}{\omega_0 C \sqrt{3}} \quad (24)$$

For a lumped low-pass π -type matching circuit with $R_L > R$ and $Q = \omega_0 C_{out} R$,

$$Q_L = \sqrt{\frac{R_L}{R} (1 + Q^2)} - 1 \quad (25)$$

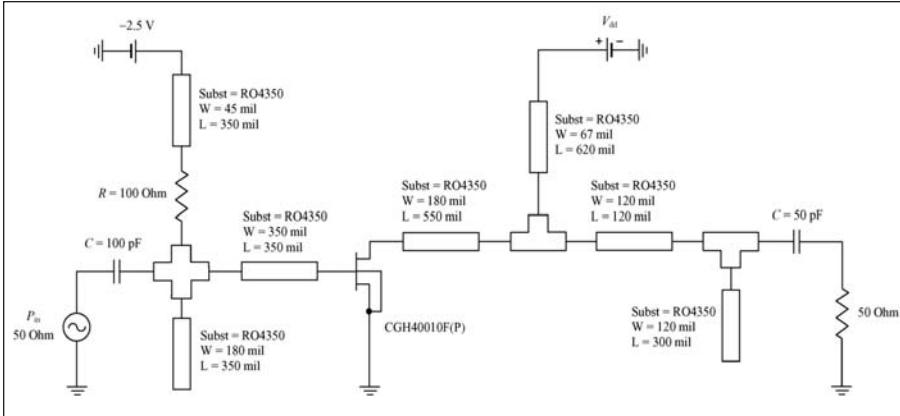


Figure 13 . Circuit schematic of transmission-line inverse Class F GaN HEMT power amplifier.

$$C = \frac{Q_L}{\omega_0 R_L} \quad (26)$$

$$L = \frac{Q + Q_L}{1 + Q_L^2} R_L \quad (27)$$

where the parameters L_{out} , C_{out} , R , and R_L are fixed [22]. By subsequent calculation of the load quality factor Q_L from Eq. (25) and then the capacitance C from Eq. (26), the characteristic impedance Z_2 can be directly obtained from Eq. (24). After calculating the inductance L from Eq. (27), the remaining parameters including the electrical lengths θ_1 and θ_2 and characteristic impedance Z_1 can be finally obtained from a system of three equations given by Eqs. (21) to (23).

Design Example

Figure 13 shows the simulated circuit schematic which approximates a transmission-line inverse Class F power amplifier based on a 28-V 10-W Cree GaN HEMT power transistor CGH40010F(P) and transmission-line load network with the second- and third-harmonic tuning, as shown in Fig. 10. The input matching circuit provides a complex-conjugate matching with the standard 50 Ω source. The load network was slightly modified by optimizing the parameters of the series trans-

mission line for implementation convenience and because of the effect of the series inductance L_{out} formed by drain bonding wires and package lead. In this case, the device input and output package leads as external elements were properly modeled to take into account the effect of their inductances, and their models were then added to the simulation setup.

Figure 14 shows the simulated results of a transmission-line inverse Class F GaN HEMT power amplifier using a nonlinear device model supplied by Cree and based on the technical parameters for a 30-mil RO4350 substrate. The maximum output power of 41.3 dBm, power gain of 13.3 dB (linear gain of about 17 dB), drain efficiency of 80.3%, and power-added efficiency (PAE) of 76.5% are achieved at an operating frequency of 2.14 GHz with a supply voltage of 28 V and a quiescent current of 40 mA.

The test board of the transmission-line inverse Class F GaN HEMT power amplifier using a 28-V 10-W Cree GaN HEMT power transistor CGH40010P in a metal-ceramic pill package was fabricated on a 30-mil RO4350 substrate. The input matching circuit, output load network, and gate and drain bias circuits (having bypass capacitors on their ends) are fully based on microstrip lines of dif-

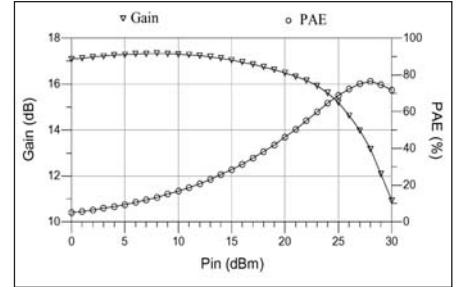


Figure 14 . Simulated results of transmission-line inverse Class F GaN HEMT power amplifier.

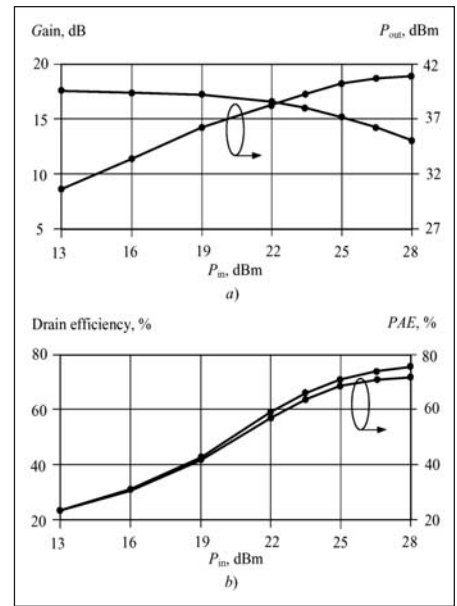


Figure 15 . Measured results of transmission-line inverse Class F power amplifier at 2.14 GHz.

ferent electrical lengths and characteristic impedances according to the simulation setup shown in Figure 13.

Figure 15 shows the measured results of a transmission-line inverse Class F GaN HEMT power amplifier which demonstrate the maximum output power of 41.0 dBm, drain efficiency of 76.0%, and PAE of 72.2% with a power gain of 13.0 dB at an operating frequency of 2.14 GHz (gate bias voltage $V_{g} = 2.8$ V, quiescent current $I_q = 50$ mA, and drain supply voltage $V_{dd} = 28$ V), achieved without any tuning of the input matching circuit and load network.

References

1. F. H. Raab, "Class-E, Class-C, and Class-F power amplifiers based upon a finite number of harmonics," *IEEE Trans. Microwave Theory Tech.*, vol. MTT-49, pp. 1462-11468, Aug. 2001.
2. A. Grebennikov and N. O. Sokal, *Switchmode RF Power Amplifiers*, Newnes, 2007.
3. V. A. Borisov and V. V. Voronovich, "Analysis of Switched-Mode Transistor Amplifier with Parallel Forming Transmission Line (in Russian)," *Radiotekhnika i Elektronika*, vol. 31, pp. 1590-1597, Aug. 1986.
4. M. K. Kazimierzczuk, "A New Concept of Class F Tuned Power Amplifier," *Proc. 27th Midwest Circuits and Systems Symp.*, pp. 425-428, 1984.
5. F. Raab, "Class-F power amplifiers with maximally flat waveforms," *IEEE Trans. Microwave Theory Tech.*, vol. MTT-45, pp. 2007-2012, Nov. 1997.
6. C. J. Wei, P. DiCarlo, Y.A. Tkachenko, R. McMorrow, and D. Bartle, "Analysis and experimental waveform study on inverse Class-F mode of microwave power FETs," *2000 IEEE MTT-S Int. Microwave Symp. Dig.*, vol. 2, pp. 525-528.
7. W. McCalpin, "High efficiency power amplification with optimally loaded harmonic waveshaping," *Proc. RF Tech. Expo'86 (Anaheim, CA)*, pp. 119-124, 1986.
8. F. Giannini and L. Scucchia, "A complete class of harmonic matching networks: synthesis and application," *IEEE Trans. Microwave Theory Tech.*, vol. MTT-57, pp. 612-619, Mar. 2009.
9. M. Helaoui and F. M. Ghannouchi, "Optimizing losses in distributed multiharmonic matching networks applied to the design of an RF GaN power amplifier with higher than 80% power-added efficiency," *IEEE Trans. Microwave Theory Tech.*, vol. MTT-57, pp. 314-322, Feb. 2009.
10. R. Negra, F. M. Ghannouchi, and W. Baechtold, "Study and design optimization of multiharmonic transmission-line load networks for Class-E and Class-F K-band MMIC power amplifiers," *IEEE Trans. Microwave Theory Tech.*, vol. MTT-55, pp. 1390-1397, June 2007.
11. K. Honjo, "A simple circuit synthesis method for microwave Class-F ultra-high-efficiency amplifiers with reactance-compensation circuits," *Int. J. Solid-State Electronics*, vol. 44, pp. 1477-1482, Aug. 2000.
12. T. Heima, A. Inoue, A. Ohta, N. Tanino, and K. Sato, "A new practical harmonics tune for high efficiency power amplifier," *Proc. 29th Europ. Microwave Conf.*, pp. 271-274, 1999.
13. P. Aflaki, R. Negra, and F. M. Ghannouchi, "Design and implementation of an inverse Class-F power amplifier with 79% efficiency by using a switch-based active device model," *Proc. 2008 IEEE Radio and Wireless Symp.*, pp. 423-426.
14. A. Grebennikov, "The frequency tuning characteristics of transistor voltage-controlled oscillators with distributed parameters," *Int. J. Circuit Theory Appl.*, vol. 27, pp. 393-414, July 1999.
15. A. Grebennikov, *RF and Microwave Transistor Oscillator Design*, John Wiley & Sons, 2007.
16. Y. Yamasaki, Y. Kittaka, H. Minamide, Y. Yamauchi, S. Miwa, S. Goto, M. Nakayama, M. Kohno, and N. Yoshida, "A 68% efficiency, C-band 100W GaN power amplifier for space applications," *2010 IEEE MTT-S Int. Microwave Symp. Dig.*, pp. 1384-1387.
17. D. H. Steinbrecher, "An interesting impedance matching network," *IEEE Trans. Microwave Theory Tech.*, vol. MTT-22, p. 382, June 1967.
18. D. Schmelzer and S. I. Long, "A GaN HEMT Class F amplifier at 2 GHz with >80% PAE," *IEEE J. Solid-State Circuits*, vol. SC-42, pp. 2130-2136, Oct. 2007.
19. S. Dietsche, C. Duvanaud, G. Pataut, and J. Obregon, "Design of high power-added efficiency FET amplifiers operating with very low drain bias voltages for use in mobile telephones at 1.7 GHz," *Proc. 23rd Europ. Microwave Conf.*, pp. 252-254, 1993.
20. A. V. Grebennikov, "Circuit design technique for high efficiency Class F amplifiers," *2000 IEEE MTT-S Int. Microwave Symp. Dig.* vol. 2, pp. 771-774.
21. A. Grebennikov, "High-efficiency transmission-line GaN HEMT inverse Class F power amplifier for active antenna arrays," *Proc. 2009 Asia-Pacific Microwave Conf.*, pp. 317-320.
22. A. Grebennikov, *RF and Microwave Power Amplifier Design*, New York: McGraw-Hill, 2004.

Author Information

Andrei Grebennikov received his Dipl. Ing. degree in radio electronics from Moscow Institute of Physics and Technology and Ph.D. degree in radio engineering from Moscow Technical University of Communications and Informatics in 1980 and 1991, respectively. He has extensive experience working with Moscow Technical University of Communications and Informatics (Russia), Institute of Microelectronics (Singapore), M/A-COM (Ireland), Infineon Technologies (Germany/Austria), and Bell Laboratories (Ireland) as an engineer, researcher, lecturer and educator. He has lectured as Guest Professor at the University of Linz (Austria) and presented short courses and tutorials as an Invited Speaker at International Microwave Symposium, European and Asia-Pacific Microwave Conferences, Institute of Microelectronics, Singapore, and Motorola Design Centre, Malaysia. He is an author and coauthor of more than 80 papers, 15 European and US patents and patent applications, and 5 books. Dr. Grebennikov can be reached at: grandrei@yahoo.com

